PERGAMON

International Journal of Non-Linear Mechanics 37 (2002) 1–18

INTERNATIONAL JOURNAL OF
NON-LINEAR
MECHANICS

www.elsevier.com/locate/ijnonlinmec

An analytic approximation of the drag coefficient for the viscous flow past a sphere

Shi-Jun Liao

School of Naval Architecture and Ocean Engineering, Shanghai Jiao Tong University, Shanghai 200030, People's Republic of China

Abstract

We give an analytic solution at the 10th order of approximation for the steady-state laminar viscous flows past a sphere in a uniform stream governed by the exact, fully non-linear Navier–Stokes equations. A new kind of analytic technique, namely the homotopy analysis method, is applied, by means of which Whitehead's paradox can be easily avoided and reasonably explained. Different from all previous perturbation approximations, our analytic approximations are valid in the whole field of flow, because we use the same approximations to express the flows near and far from the sphere. Our drag coefficient formula at the 10th order of approximation agrees better with experimental data in a region of Reynolds number $R_d < 30$, which is considerably larger than that ($R_d < 5$) of all previous theoretical ones. © 2001 Elsevier Science Ltd. All rights reserved.

Keywords: Laminar viscous flow; Sphere; Drag formula; Analytic approximations; Navier–Stokes equations; Homotopy analysis method

1. Introduction

Consider the steady-state laminar viscous flow past a sphere in a uniform stream with velocity U_∞ at infinity. Assume that the fluid is incompressible. Let a, d denote the radius and diameter of the sphere, respectively. In a spherical coordinate system whose origin is taken at the center of the sphere, the flow is governed by the Navier–Stokes equations:

$$u_r \frac{\partial u_r}{\partial r} + \frac{u_\theta}{r}\frac{\partial u_r}{\partial \theta} - \frac{u_\theta^2}{r} = -\frac{\partial p}{\partial r} + \frac{1}{R_e}\left(\nabla^2 u_r - \frac{2u_r}{r^2} - \frac{2}{r^2}\frac{\partial u_\theta}{\partial \theta} - \frac{2u_\theta \cot\theta}{r^2}\right), \tag{1.1}$$

$$u_r \frac{\partial u_\theta}{\partial r} + \frac{u_\theta}{r}\frac{\partial u_\theta}{\partial \theta} + \frac{u_r u_\theta}{r} = -\frac{1}{r}\frac{\partial p}{\partial \theta} + \frac{1}{R_e}\left(\nabla^2 u_\theta + \frac{2}{r^2}\frac{\partial u_r}{\partial \theta} - \frac{u_\theta}{r^2 \sin^2\theta}\right), \tag{1.2}$$

and the continuation equation

$$\frac{1}{r^2}\frac{\partial (r^2 u_r)}{\partial r} + \frac{1}{r\sin\theta}\frac{\partial (u_\theta \sin\theta)}{\partial \theta} = 0, \tag{1.3}$$

where u_r denotes the radial velocity, u_θ the tangential velocity, p the pressure, $R_e = aU_\infty/\nu$ the Reynolds number, ν the kinematic viscosity, respectively. All variables in the above equations are non-dimensional. On the surface of the sphere we have the non-slip conditions

$$u_r = u_\theta = 0, \quad r = 1. \tag{1.4}$$

E-mail address: sjliao@mail.sjtu.edu.cn (S.-J. Liao).

0020-7462/01/$ - see front matter
PII: S0020-7462(00)00092-5

At infinity, there exists the uniform stream condition

$$\lim_{r \to +\infty} (u_r \cos\theta - u_\theta \sin\theta) = 1. \tag{1.5}$$

Like Proudman and Pearson [11], we rewrite the above problem in a simpler way. There exists such a stream-function $\psi(r,\theta)$ satisfying

$$u_r = \frac{1}{r^2 \sin\theta} \frac{\partial\psi}{\partial\theta}, \quad u_\theta = -\frac{1}{r\sin\theta}\frac{\partial\psi}{\partial r} \tag{1.6}$$

that (1.3) is automatically satisfied. As a result, (1.1) and (1.2) can combine to yield

$$\mathscr{D}^4\psi = \frac{R_e}{r^2\sin\theta}\left(\frac{\partial\psi}{\partial\theta}\frac{\partial}{\partial r} - \frac{\partial\psi}{\partial r}\frac{\partial}{\partial\theta} + 2\cot\theta\frac{\partial\psi}{\partial r} - \frac{2}{r}\frac{\partial\psi}{\partial\theta}\right)\mathscr{D}^2\psi, \tag{1.7}$$

with non-slip conditions on the surface

$$\psi(1,\theta) = \psi_r(1,\theta) = 0, \tag{1.8}$$

and the uniform-stream condition at infinity

$$\lim_{r \to +\infty} \psi(r,\theta) = \tfrac{1}{2}r^2\sin^2\theta, \tag{1.9}$$

where the linear operators $\mathscr{D}^2$ and $\mathscr{D}^4$ are defined by

$$\mathscr{D}^2 = \frac{\partial^2}{\partial r^2} + \frac{\sin\theta}{r^2}\frac{\partial}{\partial\theta}\left(\frac{1}{\sin\theta}\frac{\partial}{\partial\theta}\right), \tag{1.10}$$

$$\mathscr{D}^4 = \left[\frac{\partial^2}{\partial r^2} + \frac{\sin\theta}{r^2}\frac{\partial}{\partial\theta}\left(\frac{1}{\sin\theta}\frac{\partial}{\partial\theta}\right)\right]^2, \tag{1.11}$$

respectively.

The non-dimensional drag coefficient C_D is defined by

$$C_D = \frac{D}{\frac{1}{2}\rho U_\infty^2 \pi a^2}, \tag{1.12}$$

where D denotes the drag of the sphere. C_D only depends upon the Reynolds number R_e. It has important physical and mathematical meanings to have a satisfactory analytic drag formula. However, this famous classical problem seems rather difficult, even today when the supercomputer has become a powerful calculation tool. The story detailing the attack of this problem is long. In 1851, neglecting completely the non-linear (inertia) term in the Navier–Stokes equations, Stokes [13] solved a set of linear partial differential equations (PDE), currently called Stokes equations, and gained his well-known drag formula

$$C_D = \frac{24}{R_d}, \tag{1.13}$$

where the Reynolds number R_d is defined by $R_d = \mathrm{d}U_\infty/\nu = 2R_e$. As shown in Fig. 1, only in a small region $R_d < 0.2$, (1.13) agrees well with the experimental data given by Maxworth [8], Ockendon and Evans [9], Roos et al. [12] and Wieselsberger [18,19]. It indicates that the non-linear terms of the Navier–Stokes equations have an important role and therefore had to be considered. In 1889, Whitehead [17] assumed an expansion of the stream function in power series of the Reynolds number and then applied straight forward perturbation techniques to this problem. However, he found that his second-order approximation remains finite at infinity in a way incompatible with the uniform-stream condition (1.9). Besides, his higher-order approximations to the velocity distribution diverge at infinity. This is currently referred to as "Whitehead paradox" in textbooks. The paradox reveals that it is impossible to apply straightforward perturbation techniques to gain a valid high-order analytic approximation for the viscous flow past a sphere. In 1910, to avoid the Whitehead paradox, Oseen [10] linearized the inertia term of the Navier–Stokes equations by using the velocity field far from the sphere. He obtained a set of linear PDEs, currently called Oseen equation in textbooks. He considered the first-term approximation of this set of PDEs and gave the famous drag formula

$$C_D = \frac{24}{R_d}\left(1 + \frac{3}{16}R_d\right). \tag{1.14}$$

In 1929, following Oseen's [10] approach, Goldstein [2] considered more terms in the solution of the Oseen equation and gained the drag formula

$$C_D = \frac{24}{R_d}\left(1 + \frac{3}{16}R_d - \frac{19}{1280}R_d^2 + \frac{71}{20{,}480}R_d^3 - \frac{30{,}179}{34{,}406{,}400}R_d^4 + \frac{122{,}519}{550{,}502{,}400}R_d^5 + \cdots\right). \tag{1.15}$$

However, both Oseen's [10] drag formula (1.14) and Goldstein's [2] drag formula (1.15) are valid only for small Reynolds number, as shown in Fig. 1. In 1970, Van Dyke [14,15] extended the above drag formula to 24 terms by computer, a new powerful calculation tool in the 20th century, and found that its convergence is limited by a simple pole at $R_d = -4.18172$. Using Euler transformation, Van Dyke [14] enlarged its convergence region to infinity. However, the agreement between Van Dyke's [14] drag formula (given by Euler transformation) with experimental data is not satisfactory for $R_d > 5$, as shown in Fig. 1. However, this disagreement is logically reasonable, because the set of *linear* Oseen equations is only a kind of approximation of the *non-linear* Navier–Stokes equations. Thus, in order to gain a better drag formula, the fully non-linear Navier–Stokes equations had to be considered. To the best of our knowledge, only a few researchers directly attacked the exact Navier–Stokes equations. In 1957, Proudman and Pearson [11] applied "matching perturbation techniques" to give a 2nd-order matched expression of outer and inner solutions. Both of their inner and outer approximations are governed by the exact Navier–Stokes equations. However, their inner approximations do not satisfy the uniform-stream condition (1.9) at infinity, while their outer approximations do not obey the non-slip condition (1.8) on the surface of the sphere. Thus, neither their inner approximations nor their outer approximations are valid in the whole field of flow. They determined unknown coefficients by matching the inner and outer approximations. In this way, Proudman and Pearson [11] proposed such a second-order drag formula

$$C_D = \frac{24}{R_d}\left[1 + \frac{3}{16}R_d + \frac{9}{160}R_d^2 \ln R_d + O(R_d^2)\right]. \tag{1.16}$$

As shown in Fig. 1, this formula is valid only in the region $R_d < 1$, and seems even worse than the Oseen formula when $R_d > 3$. In 1969, following Proudman and Pearson's [11] approach, Chester and Breach [1] gave the 3rd-order drag formula

$$C_D = \frac{24}{R_d}\left[1 + \frac{3}{16}R_d + \frac{9}{160}R_d^2\left(\ln R_d + \gamma + \frac{2}{3}\ln 2 - \frac{323}{360}\right) + \frac{27}{640}R_d^3 \ln R_d + O(R_d^3)\right], \tag{1.17}$$

where γ is the Euler constant. However, it is a little baffling that, when $R_d > 2$, the above 3rd-order drag formula is even worse than the 2nd-order formula (1.16), as shown in Fig. 1. Chester and Breach's [1] work clearly indicates that it seems meaningless to exactly follow Proudman and Pearson's [11] approach to get higher-order approximations. Notice that when $R_d > 5$ there is a large disagreement between all of above-mentioned theoretical drag formulae and experimental data. So, as pointed out by White [16] in 1991, "the idea of using creeping flow to expand into the high Reynolds number region has not been successful".

All the above-mentioned perturbation approaches are based on the assumption that the Reynolds number R_d is sufficiently small. So, it is logically reasonable and understandable that none of the above perturbation drag formulae is valid for a large Reynolds number. An obvious shortcoming of the perturbation technique is that it is too strongly dependent upon small parameter (perturbation quantity) and thus, in general, can only

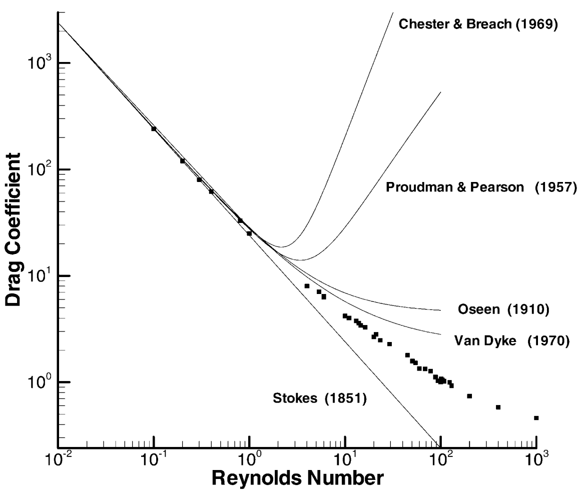

Fig. 1. Comparisons of the previous theoretical drag formulas (solid line) with experimental data (symbols) given by Roos et al. [12] and Wieselsberger [18,19]).

be applied to weakly non-linear problems. Notice that for large Reynolds number even the linear Oseen equation can give much better results than the 2nd and 3rd-order perturbation drag formulae (1.16) and (1.17). This is mainly because the Oseen equation has nothing to do with any small parameters. This might be one perfect witness that it is necessary to develop some new analytic techniques independent of small parameters.

Using the homotopy, a fundamental concept in topology, Liao [3–5] proposed such a kind of new analytic method for non-linear problems, namely the homotopy analysis method (HAM). Essentially different from perturbation techniques, the validity of the homotopy analysis method does not depend upon whether non-linear problems under consideration contain small parameters or not. Liao [3] successfully applied the homotopy analysis method to the Blasius' viscous flows. Recently, Liao [4] further applied it to gain, for the first time (to the best of our knowledge), an explicit analytic solution of the laminar viscous flow over a semi-infinite flat plate governed by the Falkner–Skan equation. Different from perturbation approximations, Liao's [4] solution for Falkner–Skan viscous flows is valid in the whole field of flow. Liao [4] showed that his 50th-order approximation converges to the numerical results of the Falkner–Skan equation quite well. Besides, the basic ideas of the homotopy analysis method have been successfully applied to propose a simple approach to enlarge the convergence region of perturbation approximations [6], and also a numerical method for strong non-linear PDEs, namely "the general boundary element method" [7]. All of these verify the validity of the homotopy analysis method. Noticing that the laminar viscous flow over a semi-infinite flat plate has a lot of the same physical characteristics as the viscous flow past a sphere in a uniform stream, we further apply the homotopy analysis method to attack this difficult classical problem. We give in this paper the 10th-order analytic approximation, which is valid in the whole field of flows. Our 10th-order drag formula agrees well with experimental data in a considerably larger region of Reynolds number than that of all the above-mentioned theoretical ones.

2. Mathematical derivations

Following Proudman and Pearson [11], we introduce the transformation

$$\mu = \cos\theta, \quad 0 \leqslant \theta \leqslant 2\pi, \tag{2.1}$$

which gives

$$\frac{\partial}{\partial\theta} = -\sin\theta\frac{\partial}{\partial\mu}. \tag{2.2}$$

Then, due to (1.10) and (1.11), the linear operators $\mathscr{D}^2$ and $\mathscr{D}^4$ become

$$\mathscr{D}^2 = \frac{\partial^2}{\partial r^2} + \frac{(1-\mu^2)}{r^2}\frac{\partial^2}{\partial\mu^2}, \tag{2.3}$$

$$\mathscr{D}^4 = \left[\frac{\partial^2}{\partial r^2} + \frac{(1-\mu^2)}{r^2}\frac{\partial^2}{\partial\mu^2}\right]^2, \tag{2.4}$$

respectively. Thus, (1.7) becomes

$$\mathscr{D}^4\psi = \frac{R_e}{r^2}\left[\frac{\partial\psi}{\partial r}\frac{\partial}{\partial\mu} - \frac{\partial\psi}{\partial\mu}\frac{\partial}{\partial r} + \frac{2\mu}{(1-\mu^2)}\frac{\partial\psi}{\partial r} + \frac{2}{r}\frac{\partial\psi}{\partial\mu}\right]\mathscr{D}^2\psi. \tag{2.5}$$

The non-slip boundary conditions are

$$\psi(r,\mu) = \psi_r(r,\mu) = 0, \quad \text{when } r = 1, \tag{2.6}$$

and the uniform stream condition becomes

$$\lim_{r\to+\infty} \psi(r,\mu) = \tfrac{1}{2}r^2(1-\mu^2), \tag{2.7}$$

where $\mu\in[-1,1]$, $r\in[1,+\infty)$ and ψ_r denotes the first-order derivatives of ψ with respect to r.

Defining a non-linear operator (Navier–Stokes operator)

$$\mathscr{A}\psi = \mathscr{D}^4\psi - \frac{R_e}{r^2}\left[\frac{\partial\psi}{\partial r}\frac{\partial}{\partial\mu} - \frac{\partial\psi}{\partial\mu}\frac{\partial}{\partial r} + \frac{2\mu}{(1-\mu^2)}\frac{\partial\psi}{\partial r} + \frac{2}{r}\frac{\partial\psi}{\partial\mu}\right]\mathscr{D}^2\psi, \tag{2.8}$$

we first of all construct a family of partial differential equations in an embedding parameter $q\in[0,1]$

and a non-zero auxiliary parameter $\hbar$ as follows:

$$(1-q)\mathscr{L}[\Psi(r,\mu,q)-\psi_0(r,\mu)] = q\hbar\mathscr{A}\Psi(r,\mu,q),$$

$$r \geqslant 1,\ -1 \leqslant \mu \leqslant 1,\ 0 \leqslant q \leqslant 1,\ \hbar \neq 0, \tag{2.9}$$

with the corresponding boundary conditions

$$\Psi(1,\mu,q) = \left.\frac{\partial \Psi(r,\mu,q)}{\partial r}\right|_{r=1} = 0,$$

$$-1 \leqslant \mu \leqslant 1,\ 0 \leqslant q \leqslant 1, \tag{2.10}$$

$$\lim_{r\to\infty} \Psi(r,\mu,q) = \tfrac{1}{2}r^2(1-\mu^2),$$

$$-1 \leqslant \mu \leqslant 1,\ 0 \leqslant q \leqslant 1, \tag{2.11}$$

where the real function $\psi_0(r,\mu)$, which satisfies the non-slip boundary conditions (2.6) and the uniform stream condition (2.7), is an initial guess approximation of $\psi(r,\mu)$; $\mathscr{L}$ is an auxiliary linear operator, $\hbar$ a non-zero auxiliary parameter, Ψ a real function of four independent variables r, μ, q and $\hbar$ (for the sake of simplicity, we do not explicitly express the relationship between Ψ and $\hbar$). It should be emphasized that we have great freedom to *select* the initial guess approximation $\psi_0(r,\mu)$, the auxiliary linear operator $\mathscr{L}$ and the value of the non-zero auxiliary parameter $\hbar$. This kind of freedom is the cornerstone of the validity of the homotopy analysis method.

When $q = 0$ and $q = 1$, we have by (2.9)–(2.11) that

$$\Psi(r,\mu,0) = \psi_0(r,\mu), \tag{2.12}$$

$$\Psi(r,\mu,1) = \psi(r,\mu), \tag{2.13}$$

respectively. Thus, the process of q increasing from zero to one is just the process of Ψ varying from $\psi_0(r,\mu)$ to $\psi(r,\mu)$. This is exactly the idea of the homotopy, and this kind of process is called deformation in topology. So, (2.9)–(2.11) are called the zeroth-order deformation equations. Obviously, (2.12) and (2.13) give a relationship between the initial guess $\psi_0(r,\mu)$ and the solution $\psi(r,\mu)$. A numerical technique, namely the continuation method, is based on it. However, this kind of relationship is indirect and therefore is useless for our analytic purpose. Thus, a direct relationship between $\psi_0(r,\mu)$ and $\psi(r,\mu)$ must be given.

Assume that the deformation $\Psi(r,\mu,q)$ is smooth enough about q so that all of the so-called mth-order deformation derivatives

$$\psi_0^{[m]}(r,\mu) = \left.\frac{\partial^m \Psi(r,\mu,q)}{\partial q^m}\right|_{q=0}, \quad m \geqslant 1, \tag{2.14}$$

exist. Then, by the Taylor series, we have

$$\Psi(r,\mu,q) = \Psi(r,\mu,0) + \sum_{m=1}^{+\infty} \frac{\psi_0^{[m]}(r,\mu)}{m!} q^m. \tag{2.15}$$

Writing

$$\psi_m(r,\mu) = \frac{\psi_0^{[m]}(r,\mu)}{m!}, \tag{2.16}$$

we have by (2.12) that

$$\Psi(r,\mu,q) = \psi_0(r,\mu) + \sum_{m=1}^{+\infty} \psi_m(r,\mu) q^m. \tag{2.17}$$

Assuming that the initial guess approximation $\psi_0(r,\mu)$, the auxiliary linear operator $\mathscr{L}$ and the auxiliary non-zero parameter $\hbar$ are so properly selected that the above Taylor series is convergent at $q = 1$, we further have by (2.13) that

$$\psi(r,\mu) = \psi_0(r,\mu) + \sum_{m=1}^{+\infty} \psi_m(r,\mu). \tag{2.18}$$

The above expression gives a direct relationship between the initial guess approximation $\psi_0(r,\mu)$ and the solution $\psi(r,\mu)$ of (2.5)–(2.7) through the unknown terms $\psi_m(r,\mu)$ ($m = 1, 2, 3, \ldots$), whose governing equations will be given below.

Differentiating the zeroth-order deformation equations (2.9)–(2.11) m times with respect to q, then setting $q = 0$, and finally dividing it by $m!$, we obtain the so-called mth-order deformation equations

$$\mathscr{L}[\psi_m(r,\mu)] = G_m(r,\mu), \quad m \geqslant 1,\ r \geqslant 1,$$

$$-1 \leqslant \mu \leqslant 1, \tag{2.19}$$

with the boundary conditions

$$\psi_m(1,\mu) = \left.\frac{\partial \psi_m(r,\mu)}{\partial r}\right|_{r=1} = 0, \quad m \geqslant 1,$$

$$-1 \leqslant \mu \leqslant 1 \tag{2.20}$$

and

$$\lim_{r\to+\infty} r^{-2}\psi_m(r,\mu) = 0, \quad m \geqslant 1, \quad -1 \leqslant \mu \leqslant 1, \tag{2.21}$$

respectively, where the right-hand side term $G_m(r,\mu)$ is given by

$$\begin{aligned} G_m(r,\mu) = {} & (\chi_m \mathscr{L} + \hbar\mathscr{D}^4)\psi_{m-1} \\ & - \frac{\hbar R_e}{r^2}\sum_{k=0}^{m-1}\left[\frac{\partial\psi_k}{\partial r}\frac{\partial}{\partial\mu} - \frac{\partial\psi_k}{\partial\mu}\frac{\partial}{\partial r}\right. \\ & \left. + \frac{2\mu}{(1-\mu^2)}\frac{\partial\psi_k}{\partial r} + \frac{2}{r}\frac{\partial\psi_k}{\partial\mu}\right]\mathscr{D}^2\psi_{m-1-k} \end{aligned} \tag{2.22}$$

and the coefficient χ_m is defined by

$$\chi_m = \begin{cases} 0 & \text{when } m \leqslant 1, \\ 1 & \text{when } m \geqslant 2. \end{cases} \tag{2.23}$$

It should be emphasized that *all* of the foregoing mth-order deformation equations (2.19)–(2.21) are *linear* partial differential equations. Thus, through (2.18), our approach transfers the original *non-linear* equations (2.5)–(2.7) into an *infinite* sequence of *linear* sub-problems. Notice that perturbation techniques use small parameters to fulfill such a kind of transformation. However, our approach does *not* need the so-called small parameter assumption at all. This is the essential reason why our results can be valid for large Reynolds number.

The essence to give analytic approximations of (2.5)–(2.7) is to express the solution $\psi(r,\mu)$ by a complete set of functions (base functions), which should be consistent with boundary conditions (2.6) and (2.7) and also with the physical natures of the problem. Besides, to ensure the validity of the proposed approach, it is important to make the series (2.18) convergent. Obviously, the convergence of the series (2.18) depends upon the initial guess $\psi_0(r,\mu)$, the auxiliary linear operator $\mathscr{L}$ and the auxiliary non-zero parameter $\hbar$. Fortunately, as mentioned above, the homotopy analysis method provides us with great freedom to select all of them. Thus, we can select a proper set of base functions to express the solution, and at the same time to ensure the convergence of (2.18). It is also this kind of freedom that provides us with the possibility to avoid the Whitehead [17] paradox in a rather simple way.

The initial guess $\psi_0(r,\mu)$ must satisfy (2.6) and (2.7). The simplest one is the Stokes solution

$$\psi_0(r,\mu) = \frac{1}{4}\left(2r^2 - 3r + \frac{1}{r}\right)(1-\mu^2). \tag{2.24}$$

Notice that (2.5) contains the linear operator $\mathscr{D}^4$. So, it seems natural, although it might be not the best, to use

$$\mathscr{L} = H(r,\mu)\mathscr{D}^4 = H(r,\mu)\left[\frac{\partial^2}{\partial r^2} + \frac{(1-\mu^2)}{r^2}\frac{\partial^2}{\partial\mu^2}\right]^2 \tag{2.25}$$

as our auxiliary linear operator, where $H(r,\mu)$ is a non-zero real function. In this way, $H(r,\mu)$ completely determines $\mathscr{L}$ so that its selection becomes very important.

Considering the boundary conditions (2.6) and (2.7), the form of the initial guess (2.24), and besides the symmetry of the flow, it is reasonable to assume that $\psi(r,\mu)$ can be expressed by trigonometric functions (base functions) in such a form that

$$\psi(r,\mu) = (1-\mu^2)\sum_{k=0}^{+\infty} F_k(r)\mu^k, \tag{2.26}$$

where $F_k(r)$ are unknown real functions and $\mu = \cos\theta$. To ensure this, we should select a proper auxiliary function $H(r,\mu)$ so that each solution $\psi_m(r,\mu)$ of (2.19)–(2.21) exists and can be expressed in the form

$$\psi_m(r,\mu) = (1-\mu^2)\sum_{k=0}^{N} f_{m,k}(r)\mu^k, \tag{2.27}$$

where N might be infinity and $f_{m,k}(r)$ are unknown real functions.

The above-mentioned approach is valid, only if both $H(r,\mu)$ and $\hbar$ are so properly selected that

(a) there exist solutions for *all* of the mth-order ($m \geqslant 1$) deformation equations (2.19)–(2.21);
(b) the series (2.18) converges to the solution of (2.5)–(2.7).

If (a) holds, one can get $\psi_1(r,\mu), \psi_2(r,\mu), \psi_3(r,\mu), \ldots$, one after the other in order by solving

(2.19)–(2.22) subsequently. Obviously, the simplest form of $H(r,\mu)$ is $H(r,\mu)=1$, corresponding to $\mathscr{L}=\mathscr{D}^4$. However, when $H(r,\mu)=1$, we gain by solving the first-order ($m=1$) deformation equations (2.19) and (2.20) that

$$\psi_1(r,\mu)=\frac{3}{32}\hbar R_e\left(2r^2-3r+1-\frac{1}{r}+\frac{1}{r^2}\right)\times(1-\mu^2)\mu, \tag{2.28}$$

which, unfortunately, does not satisfy the boundary condition (2.21) at infinity. Notice that, when $\hbar=-1$, (2.28) becomes exactly Whitehead's [17] second-order approximation, whose first-order approximation is the same as our initial approximation (2.24), i.e. Stokes solution. Therefore, (2.19)–(2.21) have no solution if we *select* $H(r,\mu)=1$. Fortunately, for the homotopy analysis method, $H(r,\mu)=1$ is just *one* among an *infinite* number of possibilities, because we have great freedom to *select* or *define* other auxiliary linear operators $\mathscr{L}$ by setting a new $H(r,\mu)$ better than $H(r,\mu)=1$. For example, we can simply *select* or *define*

$$H(r,\mu)=r^\sigma, \tag{2.29}$$

where σ is a real number. We find that, when $\sigma\leqslant 0$, (2.19)–(2.20) have no solutions satisfying the uniform-stream condition (2.21) at infinity. Thus, all non-positive values of σ will lead to the Whitehead paradox. This might give a new kind of explanation of the Whitehead paradox. However, it is very interesting that, when $\sigma>0$, there exists the solution $\psi_m(r,\mu)$ for all of the mth-order ($m\geqslant 1$) deformation equations (2.19)–(2.21), which can be simply expressed by

$$\psi_m(r,\mu)=(1-\mu^2)\sum_{k=0}^{m} f_{m,k}(r)\mu^k, \quad m\geqslant 1, \tag{2.30}$$

where $f_{m,k}(r)$ ($0\leqslant k\leqslant m$) are unknown real functions. Substituting the above *model expression* into (2.19)–(2.21), we *deduce* the governing equations

$$\begin{aligned} &r^4 f^{(4)}_{m,k}(r)-(k+1)(k+2)[2r^2 f''_{m,k}(r)-4rf'_{m,k}(r)\\ &-(k-1)(k+4)f_{m,k}(r)]\\ &\quad = Q_{m,k}(r), \quad r\geqslant 1,\ m\geqslant 1,\ 0\leqslant k\leqslant m, \end{aligned} \tag{2.31}$$

with the boundary conditions on the surface of the sphere

$$f_{m,k}(1)=f'_{m,k}(1)=0, \quad m\geqslant 1,\ 0\leqslant k\leqslant m \tag{2.32}$$

and the boundary condition at infinity

$$\lim_{r\to+\infty} r^{-2} f_{m,k}(r)=0, \quad m\geqslant 1,\ 0\leqslant k\leqslant m \tag{2.33}$$

where the right-hand side term $Q_{m,k}(r)$ in (2.31) is given by

$$\begin{aligned} Q_{m,k}(r)=\ & r^{4-\sigma}E_{m,k}(r)-2\lambda_{m,k+2}(k+1)(k+2)\\ &\times[r^2 f''_{m,k+2}(r)-2rf'_{m,k+2}(r)]\\ &-(k+1)(k+2)(k+4)\\ &\times[(k+3)\lambda_{m,k+4}f_{m,k+4}(r)\\ &-2(k+1)\lambda_{m,k+2}f_{m,k+2}(r)]. \end{aligned} \tag{2.34}$$

The real function $E_{m,k}(r)$ in (2.34) reads

$$\begin{aligned} E_{m,k}(r)=\ &(\hbar+\chi_m r^\sigma)\lambda_{m-1,k}B_{m-1,k}(r)\\ &-\frac{\hbar R_e}{r^2}\sum_{j=0}^{m-1}\left(\sum_{i=\max\{0,k+j+1-m\}}^{\min\{j+1,k\}}\right.\\ &\times C_{j,i}(r)A_{m-1-j,k-i}(r)\\ &+\sum_{i=\max\{0,k+j-m\}}^{\min\{j,k\}}[f'_{ji}(r)T_{m-1-j,k-i}(r)\\ &\left.-A'_{ji}(r)S_{m-1-j,k-i}(r)]\right) \end{aligned} \tag{2.35}$$

where

$$A_{m,k}(r)=f''_{m,k}(r)+\frac{(k+1)(k+2)}{r^2}\times[\lambda_{m,k+2}f_{m,k+2}(r)-f_{m,k}(r)], \tag{2.36}$$

$$\begin{aligned} B_{m,k}(r)=\ & f^{(4)}_{m,k}(r)+\frac{2(k+1)(k+2)}{r^2}\\ &\times[\lambda_{m,k+2}f''_{m,k+2}(r)-f''_{m,k}(r)]\\ &-\frac{4(k+1)(k+2)}{r^3}\\ &\times[\lambda_{m,k+2}f'_{m,k+2}(r)-f'_{m,k}(r)]\\ &-\frac{(k^2-1)(k+2)(k+4)}{r^4} \end{aligned}$$

$$\times[\lambda_{m,k+2} f_{m,k+2}(r) - f_{m,k}(r)] + \frac{(k+1)(k+2)(k+3)(k+4)}{r^4} \times[\lambda_{m,k+4} f_{m,k+4}(r) - \lambda_{m,k+2} f_{m,k+2}(r)], \quad (2.37)$$

$$C_{m,k}(r) = 2\left[\lambda_{m,k-1}\frac{\mathrm{d}f_{m,k-1}(r)}{\mathrm{d}r} + \frac{S_{m,k}(r)}{r}\right], \quad 0 \leqslant k \leqslant m+1, \quad (2.38)$$

$$S_{m,k}(r) = (k+1)[\lambda_{m,k+1} f_{m,k+1}(r) - \lambda_{m,k-1} f_{m,k-1}(r)], \quad 0 \leqslant k \leqslant m+1, \quad (2.39)$$

$$T_{m,k}(r) = (k+1)[\lambda_{m,k+1} A_{m,k+1}(r) - \lambda_{m,k-1} A_{m,k-1}(r)], \quad 0 \leqslant k \leqslant m+1, \quad (2.40)$$

and the coefficient $\lambda_{m,k}$ is defined by

$$\lambda_{m,k} = \begin{cases} 1 & 0 \leqslant k \leqslant m, \\ 0 & \text{otherwise.} \end{cases} \quad (2.41)$$

The detailed mathematical derivations are given in Appendix A. Notice that $f^{(4)}_{m,k}(r)$ in (2.31) denotes the 4th-order derivative of $f_{m,k}(r)$ with respect to r. Actually, (2.31) is a well-known *ordinary* differential equation, called Euler equation, which is much easier to solve than the *partial* differential equation (2.19). The corresponding homogeneous Euler equation

$$r^4 \bar{f}^{(4)}_{m,k} - (k+1)(k+2)[2r^2 \bar{f}''_{m,k} - 4r\bar{f}'_{m,k} - (k-1)(k+4)\bar{f}_{m,k}] = 0, \quad (2.42)$$

has the general solution

$$\bar{f}_{m,k}(r) = C_1 r^{-k+1} + C_2 r^{-k-1} + C_3 r^{k+2} + C_4 r^{k+4}, \quad 0 \leqslant k \leqslant m, \quad (2.43)$$

where C_1, C_2, C_3, C_4 are integral coefficients. The general solution of (2.31) is

$$f_{m,k}(r) = C_1 r^{-k+1} + C_2 r^{-k-1} + C_3 r^{k+2} + C_4 r^{k+4} + f^*_{m,k}(r), \quad (2.44)$$

where $f^*_{m,k}(r)$ is one of its special solutions. If

$$\lim_{r\to+\infty} r^{-2} f^*_{m,k}(r) = 0, \quad m \geqslant 1,\ 0 \leqslant k \leqslant m, \quad (2.45)$$

we have by (2.33) that $C_3 = C_4 = 0$. By (2.32), we further have

$$C_1 = -\tfrac{1}{2}[f^{*'}_{m,k}(1) + (k+1) f^*_{m,k}(1)], \quad (2.46)$$

$$C_2 = \tfrac{1}{2}[f^{*'}_{m,k}(1) + (k-1) f^*_{m,k}(1)]. \quad (2.47)$$

So, if (2.45) holds, the integral coefficients C_1, C_2, C_3, C_4 can be uniquely determined so that the solution of (2.31)–(2.33) exists. Thus, solving the set of linear ordinary differential equations (2.31)–(2.33) one after the other in order

$$f_{m,m}(r), f_{m,m-1}(r), f_{m,m-2}(r), \ldots, f_{m,2}(r), f_{m,1}(r), f_{m,0}(r),$$

where $m = 1, 2, 3, \ldots$, we can obtain all of these solutions, subsequently. Our symbolic computations verify that (2.45) indeed holds if $\sigma > 0$.

Although for any $\sigma > 0$ there exist solutions to all of the mth-order deformation equations (2.19)–(2.21), the validity of the current approach still depends upon whether or not the series (2.18) converges to the solution of (2.5)–(2.7). Currently, Liao [5] proved for rather general non-linear PDEs that *any* infinite series given by the homotopy analysis method is definitely one of the solutions of the considered non-linear problems as long as it is convergent. Analogously, we can prove such a theorem that

Convergence Theorem. *Let* $\mathscr{L} = H(r,\mu)\mathscr{D}^4$ *denote the auxiliary linear operator, where* $\mathscr{D}^4$ *is defined by* (2.4) *and* $H(r,\mu)$ *is a non-zero real function. Assume that* $H(r,\mu)$ *is so properly selected that* (2.31)–(2.33) *have solutions for all* $m \geqslant 1$. *Then, if the corresponding series* (2.18) *is convergent, it must converge to the solution of the original equations* (2.5)–(2.7).

Considering the length of this paper, we do not repeat the proof here. For details, please refer to Liao [5]. Due to this theorem, we only need to focus on ensuring the convergence of the series (2.18) by selecting proper values of σ and $\hbar$.

3. Drag coefficient C_D

Following Chester and Breach [1], we write the drag in the form

$$D = 2\pi\rho v a U_\infty \int_0^\pi \left[-p\cos\theta + \frac{\partial^2\psi}{\partial r^2} \right]\Bigg|_{r=1} \sin\theta \, d\theta, \tag{3.1}$$

where the pressure p is given by

$$p = -\int_0^\theta \frac{\partial^3\psi}{\partial r^3}\Bigg|_{r=1} \frac{d\theta}{\sin\theta} = -\int_\mu^1 \frac{\partial^3\psi}{\partial r^3}\Bigg|_{r=1} \frac{d\mu}{(1-\mu^2)}. \tag{3.2}$$

According to (1.12), the drag coefficient is

$$C_D = \frac{4}{R_e}\int_{-1}^{+1} \left[-p\mu + \frac{\partial^2\psi}{\partial r^2} \right]\Bigg|_{r=1} d\mu. \tag{3.3}$$

By (2.30), the mth-order approximation of ψ can be rewritten as

$$\psi(r,\mu) \approx \sum_{k=0}^{m} (1-\mu^2) \sum_{i=0}^{k} f_{k,i}(r)\mu^i$$
$$= (1-\mu^2)\sum_{i=0}^{m} \mu^i \sum_{k=i}^{m} f_{k,i}(r). \tag{3.4}$$

Substituting (3.4) into (3.2) gives

$$p = -\sum_{i=0}^{m} \frac{(1-\mu^{i+1})}{(i+1)} \sum_{k=i}^{m} f'''_{m,i}(1). \tag{3.5}$$

Substituting (3.4) and (3.5) into (3.3), we have the mth-order drag coefficient

$$C_D = \frac{4}{R_e}\sum_{i=0}^{m} \frac{[1+(-1)^i]}{(i+1)(i+3)} \sum_{k=i}^{m} [2f''_{k,i}(1) - f'''_{k,i}(1)]. \tag{3.6}$$

Notice that (3.6) is valid for any $H(r,\mu) = r^\sigma$ when $\sigma > 0$.

4. High-order approximate solutions

The mathematical expressions and the convergence theorem given in the above sections hold for any $\sigma > 0$ and $\hbar \neq 0$. As pointed out in Section 2, in case of

$$\mathscr{L} = r^\sigma\left[\frac{\partial^2}{\partial r^2} + \frac{(1-\mu^2)}{r^2}\frac{\partial^2}{\partial\mu^2} \right],$$

(2.19)–(2.21) have solutions if and only if $\sigma > 0$. So, the value of σ is important for the solution of (2.19)–(2.21). However, the convergence of (2.18) is determined by both σ and $\hbar$. Thus, one can first select a reasonable value $\sigma > 0$ to ensure that (2.31)–(2.33) have solutions, and then find a proper value of $\hbar$ to enforce (2.18) convergent.

For the sake of simplicity, we set $\sigma = 1$ in all the following parts of this paper. Therefore, we virtually use

$$\mathscr{L} = r\left[\frac{\partial^2}{\partial r^2} + \frac{(1-\mu^2)}{r^2}\frac{\partial^2}{\partial\mu^2} \right]^2$$

as our auxiliary linear operator. Noticing that Stokes solution (2.24) is used as our initial guess approximation, we have by (2.30) that

$$f_{0,0}(r) = \tfrac{1}{4}(2r^2 - 3r + 1/r). \tag{4.1}$$

Then, solving the set of ordinary differential equations (2.31)–(2.33) one after the other in order by means of MATHEMATICA (version 3.0), we get the corresponding solutions at 10th-order approximation

$$f_{1,1}(r) = \hbar R_e\left[\frac{3}{16}r - \frac{9}{40}\left(\ln r + \frac{19}{28}\right) - \frac{1}{280}\left(9\ln r + \frac{39}{4}\right)\frac{1}{r^2} \right], \tag{4.2}$$

$$f_{1,0}(r) = 0, \tag{4.3}$$

$$f_{2,2}(r) = \hbar^2 R_e^2\left[\left(\frac{411}{4480} + \frac{3\ln r}{32}\right) - \frac{3}{80}r + \frac{3}{512}\frac{1}{r^2} + \frac{1}{1792}\frac{1}{r^5} + \left(\frac{873{,}401}{131{,}712{,}000} - \frac{1931\ln r}{329{,}280} - \frac{3\ln^2 r}{392}\right)\frac{1}{r^3} - \left(\frac{8{,}862{,}851}{131{,}712{,}000} - \frac{32{,}643\ln r}{392{,}000} - \frac{243\ln^2 r}{2800}\right)\frac{1}{r} \right], \tag{4.4}$$

$$f_{2,1}(r) = \hbar R_e\left[\frac{3}{16}r - \frac{9}{40}\left(\ln r + \frac{19}{28}\right) - \frac{1}{280}\left(9\ln r + \frac{39}{4}\right)\frac{1}{r^2}\right], \tag{4.5}$$

$$\begin{aligned} f_{2,0}(r) = \hbar^2 R_e^2\Bigg[&\left(\frac{69}{4480} - \frac{3\ln r}{160}\right) - \left(\frac{5{,}784{,}539}{164{,}640{,}000} - \frac{3\ln r}{80}\right)r \\ &+ \left(\frac{15{,}997{,}487}{658{,}560{,}000} + \frac{603\ln r}{19{,}600} + \frac{27\ln^2 r}{1120}\right)\frac{1}{r} - \frac{29}{3584}\frac{1}{r^2} \\ &+ \left(\frac{2{,}343{,}919}{658{,}560{,}000} + \frac{3517\ln r}{823{,}200} + \frac{3\ln^2 r}{1960}\right)\frac{1}{r^3} - \frac{1}{37{,}632}\frac{1}{r^5}\Bigg], \end{aligned} \tag{4.6}$$

and so on. All of them are valid in the whole field of flow. Unfortunately, unlike our previous publications [4,5], we fail to give higher-order approximations, because, due to the non-linearity of $Q_{m,k}$ in (2.31), the terms of $f_{m,k}(r)$ increase almost exponentially. Thus, when solving the 11th-order approximation, the symbolic computational software MATHEMATICA (version 3.0) exits because of "out of memory".

Notice that, due to (4.2)–(4.6),

$$\begin{aligned} \psi_2(r,\mu) &= (1-\mu^2)[\mu^2 f_{2,2}(r) + \mu f_{2,1}(r) + f_{2,0}(r)] \\ &= \sin^2\theta[f_{2,2}(r)\cos^2\theta + f_{2,1}(r)\cos\theta + f_{2,0}(r)] \end{aligned}$$

contains both the first-order term $O(R_e)$ and the second-order term $O(R_e^2)$, if we consider R_e as a small parameter. In general, all solutions of $\psi_m(r,\mu)$ $(m \geqslant 2)$ have such a nature. This clearly indicates that the approximations given by the proposed homotopy analysis method are in essence rather different from perturbation ones. Therefore, our approach indeed contains something essentially different.

By (3.6), we obtain
the 1st-order drag formula:

$$C_D = \frac{24}{R_d}, \tag{4.7}$$

the 2nd-order drag formula:

$$C_D = \frac{24}{R_d}\left[1 + \frac{2{,}307{,}989}{493{,}920{,}000}(\hbar R_d)^2\right], \tag{4.8}$$

the 3rd-order drag formula:

$$C_D = \frac{24}{R_d}\left[1 + \left(\frac{2{,}307{,}989}{164{,}640{,}000} + \frac{10{,}781}{7{,}840{,}000}\hbar\right)(\hbar R_d)^2\right], \tag{4.9}$$

the 4th-order drag formula:

$$\begin{aligned} C_D = \frac{24}{R_d}\Bigg[1 &+ \left(\frac{2{,}307{,}989}{82{,}320{,}000} + \frac{10{,}781}{1{,}960{,}000}\hbar + \frac{20{,}569{,}489}{52{,}157{,}952{,}000}\hbar^2\right)(\hbar R_d)^2. \\ &- \frac{33{,}257{,}111{,}326{,}660{,}589{,}843}{921{,}907{,}325{,}892{,}833{,}280{,}000{,}000}(\hbar R_d)^4\Bigg], \end{aligned} \tag{4.10}$$

the 5th-order drag formula:

$$\begin{aligned} C_D = \frac{24}{R_d}[1 &+ (4.6727992387\times 10^{-2} \\ &+ 1.37512755102\times 10^{-2}\hbar \\ &+ 1.9718459229\times 10^{-3}\hbar^2 \\ &+ 5.0611744367\times 10^{-5}\hbar^3)(\hbar R_d)^2 \\ &- (1.8037122817\times 10^{-4} \\ &+ 1.8263042456\times 10^{-6}\hbar)(\hbar R_d)^4], \end{aligned} \tag{4.11}$$

the 6th-order drag formula:

$$\begin{aligned} C_D = \frac{24}{R_d}[1 &+ (7.0091988581\times 10^{-2} \\ &+ 2.7502551020\times 10^{-2}\hbar \\ &+ 5.9155377688\times 10^{-3}\hbar^2 \\ &+ 3.0367046620\times 10^{-4}\hbar^3 \\ &- 7.6656497427\times 10^{-5}\hbar^4)(\hbar R_d)^2 \end{aligned}$$

$$- (5.4111368452 \times 10^{-4} + 1.0957825474 \times 10^{-5}\hbar - 2.9697166816 \times 10^{-6}\hbar^2)(\hbar R_d)^4 + 3.4592786538 \times 10^{-7}(\hbar R_d)^6], \tag{4.12}$$

the 7th-order drag formula:

$$C_D = \frac{24}{R_d}[1 + (9.8128784014 \times 10^{-2} + 4.8129464286 \times 10^{-2}\hbar + 1.3802921461 \times 10^{-2}\hbar^2 + 1.0628466317 \times 10^{-3}\hbar^3 - 5.3659548199 \times 10^{-4}\hbar^4 - 1.2116889029 \times 10^{-4}\hbar^5)(\hbar R_d)^2 - (1.2625985972 \times 10^{-3} + 3.8352389157 \times 10^{-5}\hbar - 2.0788016771 \times 10^{-5}\hbar^2 - 2.2155334561 \times 10^{-6}\hbar^3)(\hbar R_d)^4 + (2.4214950576 \times 10^{-6} - 1.3363946031 \times 10^{-7}\hbar)(\hbar R_d)^6], \tag{4.13}$$

the 8th-order drag formula:

$$C_D = \frac{24}{R_d}[1 + (1.3083837868 \times 10^{-1} + 7.7007142857 \times 10^{-2}\hbar + 2.7605842921 \times 10^{-2}\hbar^2 + 2.8342576846 \times 10^{-3}\hbar^3 - 2.1463819280 \times 10^{-3}\hbar^4 - 9.6935112232 \times 10^{-4}\hbar^5 - 1.3201756733 \times 10^{-4}\hbar^6)(\hbar R_d)^2 - (2.5251971944 \times 10^{-3} + 1.0227303775 \times 10^{-4}\hbar - 8.3152067084 \times 10^{-5}\hbar^2 + 1.7724267649 \times 10^{-6}\hbar^3 - 8.4707438362 \times 10^{-7}\hbar^4)(\hbar R_d)^4 + (9.6859802306 \times 10^{-6} - 1.0691156825 \times 10^{-6}\hbar + 1.0050877501 \times 10^{-7}\hbar^2)(\hbar R_d)^6 - 2.902542179 \times 10^{-9}(\hbar R_d)^8], \tag{4.14}$$

the 9th-order drag formula:

$$C_D = \frac{24}{R_d}[1 + (1.6822077259 \times 10^{-1} + 1.1551071429 \times 10^{-1}\hbar + 4.9690517258 \times 10^{-2}\hbar^2 + 6.3770797902 \times 10^{-3}\hbar^3 - 6.4391457839 \times 10^{-3}\hbar^4 - 4.3620800504 \times 10^{-3}\hbar^5 - 1.1881581060 \times 10^{-3}\hbar^6 - 1.2897570146 \times 10^{-4}\hbar^7)(\hbar R_d)^2 - (4.5453549500 \times 10^{-3} + 2.3011433494 \times 10^{-4}\hbar - 2.4945620125 \times 10^{-4}\hbar^2 - 7.9759204420 \times 10^{-5}\hbar^3 - 7.6236694526 \times 10^{-6}\hbar^4 + 1.9439178298 \times 10^{-7}\hbar^5)(\hbar R_d)^4 + (2.9057940692 \times 10^{-5} - 4.8110205711 \times 10^{-6}\hbar - 9.0457897508 \times 10^{-7}\hbar^2 - 3.472100933 \times 10^{-8}\hbar^3)(\hbar R_d)^6 - (2.6122879611 \times 10^{-8} - 3.6188982494 \times 10^{-9}\hbar)(\hbar R_d)^8]. \tag{4.15}$$

In fact, all of our drag formulae can be expressed in a general form

$$C_D = \frac{24}{R_d}\left(1 + \sum_{q=1}^{\omega(m,0)} \sum_{l=2q}^{m} \kappa_m^{q,l} R_d^{2q} \hbar^l\right), \tag{4.16}$$

where $\kappa_m^{q,l}$ are constant coefficients and the integer function $\omega(m,n)$ is defined as "taking the integer part of $(m-n)/2$". The numerical values (in the 32 decimal accuracy) of the coefficients $\kappa_m^{q,l}$ of the 10th-order drag approximation are listed in Appendix B.

Similar to Liao's [3,4] previous results for Blasius' and Falkner–Skan's viscous flow, the convergence region of the series (3.6) depends on $\hbar$. It is interesting that there always exists a region of $\hbar$, in which a series given by the homotopy analysis method is convergent, as reported by Liao [3–5]. For Blasius' flow, Liao's [3] solution is convergent in a region $-5.69 \leqslant \eta \leqslant +5.69\sqrt[3]{2|\hbar|^{-1}-1}$, where $|1+\hbar|<1$. This region tends to infinity as $\hbar$ ($\hbar<0$) tends to zero. For Falkner–Skan's flow, Liao's [4] 50th-order approximation converges in the whole field of flow when $-1 \leqslant \hbar < 0$. All of our previous publications verify that such a region of $\hbar$ can be found as long as approximations at high enough order can be gained. However, in this paper we fail to get approximations higher than 10th-order. Therefore, we cannot exactly determine such a region of $\hbar$ for our drag coefficient series (3.6). What we can do is to attempt some values of $\hbar$ and then to compare them with experimental data. First of all, we set $\hbar=-1$ and find that the 10th-order drag formula is invalid when $R_d>5$. Then, recalling our previous experience in Blasius and Falkner–Skan flows, we attempt some negative values of $\hbar$ closer to zero. In case of $\hbar=-1/2$, the valid region of the 10th-order drag formula increases to $R_d<9$, and in case of $\hbar=-1/3$, it further increases to $R_d<20$, as shown in Fig. 2. Thus, the convergence region of our drag formulae seems to increase as $\hbar(\hbar<0)$ approaches zero. In our previous applications of the homotopy analysis method, we have gained the same qualitative result, but in more rigorous mathematical meanings, by giving approximations at the 50th or even higher order. Notice that, when $\hbar=-1/3$, our 10th-order drag formula is better, in the region $R_d<20$, than all previous theoretical ones, as shown in Fig. 5. This indicates that our approach is rather promising.

In all of our previous applications of the homotopy analysis method, we regarded $\hbar$ as a constant. However, this is unnecessary. Fig. 2 clearly indicates that the value of $|\hbar|$, where $\hbar<0$, should be decreased as the Reynolds number R_d increases.

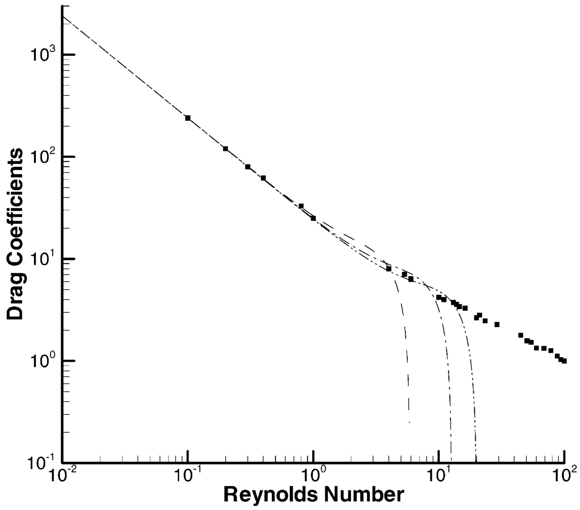

Fig. 2. Comparison of the 10th-order HAM drag formula in case $\hbar=-1$ (dashed line), $\hbar=-1/2$ (dash–dot line) and $\hbar=-1/3$ (dash–dot–dot line) with experimental data (symbols).

Thus, one can select $\hbar$ as a function of R_d. Certainly, there exist many such kinds of functions. In this paper, we only consider the following two cases:

$$\hbar=-\tfrac{1}{3}\exp(-R_d/30), \tag{4.17}$$

and

$$\hbar=-\frac{1}{1+R_d/4}. \tag{4.18}$$

In both cases, our 10th-order drag formula agrees well with experimental data in the region $R_d<30$, as shown in Figs. 3 and 4. The curves of drag coefficients at lower order of approximations are also plotted in Figs. 3 and 4, which clearly indicate that, the higher the order of approximation, the better the agreement between our drag formula and experimental data. Thus, our drag formula seems to be convergent in a large region of Reynolds number R_d, although we cannot prove it rigorously right now. This kind of tendency of convergence is very important, especially when a rigorous mathematical proof of convergence cannot be given. Comparison of our 10th-order drag formula in case of $\hbar=-1/3$, $\hbar=-\frac{1}{3}\exp(-R_d/30)$ and $\hbar=-(1+R_d/4)^{-1}$ with the previous theoretical ones is shown

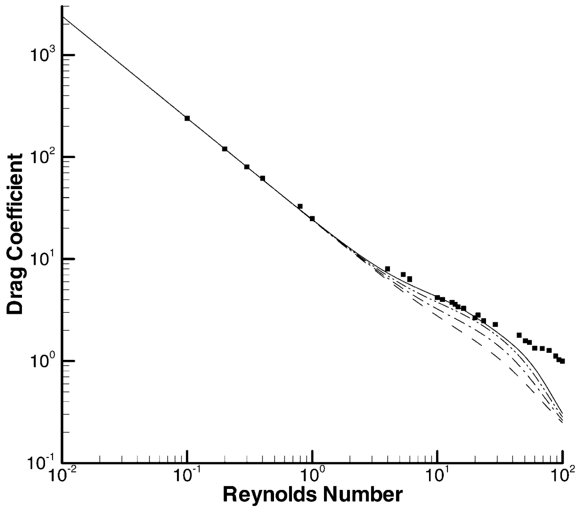

Fig. 3. Comparison of the HAM drag formulas in case $\hbar = -\frac{1}{3}\exp(-R_d/30)$ at the 4th (dash line), 6th (dash–dot line), 8th (dash–dot–dot line) and 10th-order (solid line) of approximations with experimental data (symbols).

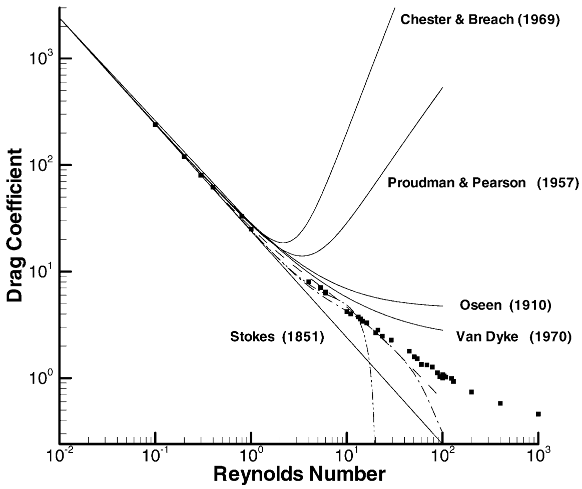

Fig. 5. Comparison of the 10th-order HAM drag formulas in case $\hbar = -1/3$ (dash–dot–dot line), $\hbar = -\frac{1}{3}\exp(-R_d/30)$ (dash–dot line) and $\hbar = -(1 + R_d/4)^{-1}$ (dash line) with the previous theoretical drag expressions (solid line) and experimental data (symbols).

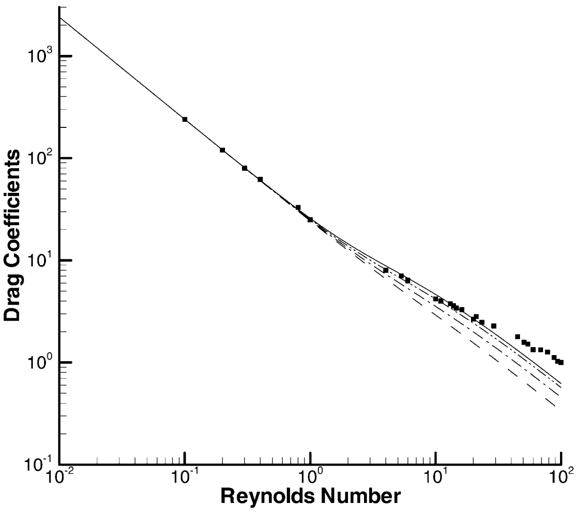

Fig. 4. Comparison of the HAM drag formulas in case $\hbar = -(1 + R_d/4)^{-1}$ at the 4th (dash line), 6th (dash–dot line), 8th (dash–dot–dot line) and 10th-order (solid line) of approximations with experimental data (symbols).

in Fig. 5. In all cases, our 10th-order drag formula agrees well with experimental data in the region $R_d < 30$, which is much larger than all previous theoretical ones. It seems that our approach might give a drag formula valid even at $R_d = 100$, if we could get high enough approximations in case of $\hbar = -(1 + R_d/4)^{-1}$. Therefore, it seems promising that our approach can give a much better analytic drag formula.

5. Conclusions and discussions

In this paper we considered the analytic approximations of the steady-state viscous flow past a sphere, an unsolved classical problem in fluid mechanics. As mentioned in Section 1, neither Whitehead's (1889) direct perturbation method nor Oseen's (1910) linear equation nor Proudman and Pearson's (1957) matching perturbation technique can give satisfactory drag formulae for large Reynolds number. None of the previous theoretical drag formulae are valid for $R_d > 5$, as shown in Fig. 1. Thus, it is valuable and beneficial to make some new attempts to attack this famous problem.

Inspired by our previous successful applications, we apply a new analytic method, namely the homotopy analysis method, to this classical problem. By selecting a proper auxiliary linear operator, we successfully transfer the exact Navier–Stokes equations into an infinite sequence of linear ordinary differential equations, which can be solved one after the other in order. Due to the complexity of the considered problem and the limitations of the current symbolic calculation software MATHEMATICA (version 3.0), we gain only 10th-order approximations, which is, however, not high enough to determine the convergence region of our drag formula. However, when the auxiliary parameter $\hbar$ is adequately selected, for example, $\hbar = -\frac{1}{3}\exp(-R_d/30)$ or $\hbar = -(1+R_d/4)^{-1}$, our 10th-order drag formula agrees well with experimental data in $R_d < 30$, a region much larger than that ($R_d < 5$) of all previous theoretical ones. Besides, as shown in Figs. 3 and 4, the higher the order of approximation, the better the agreement between our drag formulae and experimental data. This strongly suggests the convergence of our approximations in a large region of Reynolds number. Therefore, the proposed new approach seems rather promising.

The cornerstone of our approach is the freedom in selecting the auxiliary linear operator $\mathscr{L}$, the initial guess $\psi_0(r,\mu)$ and the non-zero auxiliary parameter $\hbar$. In this paper we select a special type of auxiliary linear operator

$$\mathscr{L} = r^{\sigma}\left[\frac{\partial^2}{\partial r^2} + \frac{(1-\mu^2)}{r^2}\frac{\partial^2}{\partial \mu^2}\right]^2. \tag{5.1}$$

When $\sigma \leqslant 0$, we meet Whitehead's paradox and fail to solve the whole set of the related PDEs. Fortunately, thanks to the freedom of selecting σ, Whitehead's paradox can be very easily avoided by simply setting $\sigma > 0$. For the sake of simplicity, we select $\sigma = 1$ in this paper. Notice that (5.1) is only *one* special operator among an *infinite* number of possibilities, and there might exist some better ones. At least, there are two other possibilities. One is to use the flow in the infinity, i.e. $\psi = \frac{1}{2}r^2(1-\mu^2)$, to linearize the Navier–Stokes operator (2.8). This gives such an auxiliary linear operator

$$\mathscr{L}_1\psi = \mathscr{D}^4\psi - \frac{R_e}{r}\left[(1-\mu^2)\frac{\partial}{\partial \mu} + r\mu\frac{\partial}{\partial r}\right]\mathscr{D}^2\psi. \tag{5.2}$$

The other is to use Stokes solution (2.24) to linearize (2.8), say,

$$\mathscr{L}_2\psi = \mathscr{D}^4\psi - \frac{R_e}{r}\left[\frac{\partial\psi_0}{\partial r}\frac{\partial}{\partial \mu} - \frac{\partial\psi_0}{\partial \mu}\frac{\partial}{\partial r} + \frac{3}{2}\mu\left(1-\frac{1}{r^2}\right)\right]\mathscr{D}^2\psi, \tag{5.3}$$

where ψ_0 is given by (2.24). It might be interesting to study if better drag formulae can be gained by using the above operators as the auxiliary linear operator $\mathscr{L}$. Secondly, in all of our previous applications, $\hbar$ was regarded as a constant. In this paper, by means of setting $\hbar$ as a function of the Reynolds number, such as $\hbar = -\frac{1}{3}\exp(-R_d/30)$ or $\hbar = -(1+R_d/4)^{-1}$, our 10th-order drag formula is greatly improved. It is possible that some other definitions of $\hbar$ can give even better results. Finally, in this paper we simply use Stokes solution (2.24) as our initial guess. This is however unnecessary, too. One can attempt some other functions as the initial guess $\psi_0(r,\mu)$, as long as they satisfy both (2.6) and (2.7). All of these are based on the freedom of selecting the auxiliary linear operator, the initial guess and the auxiliary non-zero parameter $\hbar$, provided by our approach. This kind of freedom provides us not only with large flexibility to apply the homotopy analysis method to many unsolved nonlinear problems but also with great potential to improve the method itself. However, on the other hand, it also brings us a lot of uncertainty, because the freedom is so large that it seems difficult to find out a better one or the best one from all of these possibilities. How to select a better auxiliary linear operator $\mathscr{L}$ and an auxiliary parameter $\hbar$ for a given problem? Is a selected initial guess the best one? Indeed, our approach puts forward new possibilities, together with new challenges at the same time, like any new method or technique at its beginning.

We do not worry about the validity of this approach, which has been proved in our previous publications [3–5]. What we are not sure about in this paper is the convergence of our approximations, which is strongly dependent upon how to *select* or *define* the initial guess $\psi_0(r,\theta)$, the auxiliary linear operator $\mathscr{L}$, the value of the non-zero parameter $\hbar$. More precisely speaking, we do not know whether or not all of them are properly *selected* or *defined* in this paper. Fortunately, even if someday one can get approximations of high enough order to prove that our approximations are divergent, it is still possible to attempt another better initial guess $\psi_0(r,\theta)$, and/or another better auxiliary linear operator $\mathscr{L}$, and/or another better value of $\hbar$, to ensure the approximate series convergent.

Despite having the above-mentioned shortcomings, our 10th-order drag formula agrees well with experimental data in a much larger region of Reynolds number than *all* previous theoretical drag expressions. Besides, the great freedom and flexibility of the proposed approach in selecting the auxiliary linear operator, the initial guess and the auxiliary non-zero parameter $\hbar$ imply huge possibility and potential to make further improvements of this approach. Thus, it puts forward a new promising way to attack this famous unsolved problem. Although about 150 yr have passed since Stokes [13] considered this problem, it is still worth attempting some new mathematical methods and new calculation tools to gain an elegant but accurate enough drag formula valid in a large enough region of Reynolds number.

Acknowledgements

Thanks to Professor Peter Hagedorn (Applied Mechanics, Darmstadt University of Technology) and the anonymous reviewers of Int. J. Non-linear Mechanics, for their valuable comments in the past several years. Special thanks go to Professor Chiang C. Mei (Department of Civil and Environmental Engineering, MIT), Professor Antonio Campo (College of Engineering, Idaho State University), Professor You-Shen He (School of Mechanical Engineering, Shanghai Jiao Tong University) and Professor Din-Yu Hsieh (Division of Applied Mathematics, Brown University), for their inspiration and encouragement.

Appendix A. Derivation of formulae related to model expression (2.30)

We prove that mode expression (2.30) holds for all non-negative integers $m \geqslant 0$.

Proof.

(I) Due to the initial guess (2.24), mode expression (2.30) holds when $m = 0$.

(II) We can prove that if mode expression (2.30) holds for $0 \leqslant l \leqslant m-1$ ($m \geqslant 1$), say,

$$\psi_l(r,\mu) = (1-\mu^2)\sum_{k=0}^{l} f_{l,k}(r)\mu^k,$$

$$0 \leqslant l \leqslant m-1, \; m \geqslant 1, \tag{A.1}$$

then it also holds for $l = m$. For $0 \leqslant l \leqslant m-1$, we have by (2.3), (2.4) and (A.1) that

$$\begin{aligned}\mathscr{D}^2\psi_l = (1-\mu^2)\Bigg\{ &\sum_{k=0}^{l} \left[f''_{l,k}(r) - (k+1)(k+2)\frac{f_{l,k}(r)}{r^2}\right]\mu^k \\ &+ \sum_{k=0}^{l-2}\left[(k+1)(k+2)\frac{f_{l,k+2}(r)}{r^2}\right]\mu^k\Bigg\}\end{aligned} \tag{A.2}$$

and

$$\begin{aligned} D^4\psi_l &= (1-\mu^2)\Bigg\{\sum_{k=0}^{l}\left[f^{(4)}_{l,k} - (k+1)(k+2)\left(\frac{2f''_{l,k}}{r^2} - \frac{4f'_{l,k}}{r^3} - (k-1)(k+4)\frac{f_{l,k}}{r^4}\right)\right]\mu^k \\ &+ \sum_{k=0}^{l-2}(k+1)(k+2)\left[\frac{f''_{l,k+2}}{r^2} - \frac{4f'_{l,k+2}}{r^3} - (k-1)(k+4)\frac{f_{l,k+2}}{r^4}\right]\mu^k \\ &+ \sum_{k=0}^{l-2}(k+1)(k+2)\left[\frac{f''_{l,k+2}}{r^2} - (k+3)(k+4)\frac{f_{l,k+2}}{r^4}\right]\mu^k \\ &+ \sum_{k=0}^{l-4}(k+1)(k+2)(k+3)(k+4)\left[\frac{f_{l,k+4}}{r^4}\right]\mu^k\Bigg\}.\end{aligned} \tag{A.3}$$

Defining

$$\lambda_{l,k} = \begin{cases} 1, & 0 \leqslant k \leqslant l, \\ 0 & \text{otherwise,}\end{cases} \tag{A.4}$$

we have for $0 \leqslant l \leqslant m-1$ that

$$\mathscr{D}^2\psi_l = (1-\mu^2)\sum_{k=0}^{l} A_{l,k}(r)\mu^k, \tag{A.5}$$

$$\mathscr{D}^4\psi_l = (1-\mu^2)\sum_{k=0}^{l} B_{l,k}(r)\mu^k, \tag{A.6}$$

respectively, where $A_{l,k}(r)$ and $B_{l,k}(r)$ $(0 \leqslant k \leqslant l)$ are defined by

$$A_{l,k}(r) = f''_{l,k}(r) + \frac{(k+1)(k+2)}{r^2} \times [\lambda_{l,k+2} f_{l,k+2}(r) - f_{l,k}(r)], \tag{A.7}$$

$$\begin{aligned} B_{l,k}(r) = f^{(4)}_{l,k}(r) &+ \frac{2(k+1)(k+2)}{r^2} \\ &\times [\lambda_{l,k+2} f''_{l,k+2}(r) - f''_{l,k}(r)] \\ &- \frac{4(k+1)(k+2)}{r^3} \\ &\times [\lambda_{l,k+2} f'_{l,k+2}(r) - f'_{l,k}(r)] \\ &- \frac{(k^2-1)(k+2)(k+4)}{r^4} \\ &\times [\lambda_{l,k+2} f_{l,k+2}(r) - f_{l,k}(r)] \\ &+ \frac{(k+1)(k+2)(k+3)(k+4)}{r^4} \\ &\times [\lambda_{l,k+4} f_{l,k+4}(r) - \lambda_{l,k+2} f_{l,k+2}(r)]. \end{aligned} \tag{A.8}$$

According to (A.1) and (A.5), we have for $0 \leqslant l \leqslant m-1$ that

$$\frac{\partial \psi_l(r,\mu)}{\partial r} = (1-\mu^2)\sum_{k=0}^{l} f'_{l,k}(r)\mu^k, \tag{A.9}$$

$$\frac{\partial}{\partial r}(\mathscr{D}^2\psi_l) = (1-\mu^2)\sum_{k=0}^{l} A'_{l,k}(r)\mu^k, \tag{A.10}$$

$$\frac{\partial \psi_l(r,\mu)}{\partial \mu} = \sum_{k=0}^{l+1} S_{l,k}(r)\mu^k, \tag{A.11}$$

$$\frac{\partial}{\partial \mu}(\mathscr{D}^2\psi_l) = \sum_{k=0}^{l+1} T_{l,k}(r)\mu^k, \tag{A.12}$$

where

$$S_{l,k}(r) = (k+1)[\lambda_{l,k+1} f_{l,k+1}(r) - \lambda_{l,k-1} f_{l,k-1}(r)], \quad 0 \leqslant k \leqslant l+1, \tag{A.13}$$

$$T_{l,k}(r) = (k+1)[\lambda_{l,k+1} A_{l,k+1}(r) - \lambda_{l,k-1} A_{l,k-1}(r)], \quad 0 \leqslant k \leqslant l+1. \tag{A.14}$$

By (A.1), we have for $0 \leqslant l \leqslant m-1$ that

$$\frac{2\mu}{(1-\mu^2)}\frac{\partial \psi_l}{\partial r} + \frac{2}{r}\frac{\partial \psi_l}{\partial \mu} = \sum_{k=0}^{l+1} C_{l,k}(r)\mu^k \tag{A.15}$$

where

$$C_{l,k}(r) = 2\left[\lambda_{l,k-1}\frac{\mathrm{d}f_{l,k-1}(r)}{\mathrm{d}r} + \frac{S_{l,k}(r)}{r}\right], \quad 0 \leqslant k \leqslant l+1. \tag{A.16}$$

Thus, by (A.15) and (A.5), it holds for $0 \leqslant k \leqslant m-1$ that

$$\begin{aligned} &\left[\frac{2\mu}{(1-\mu^2)}\frac{\partial \psi_k}{\partial r} + \frac{2}{r}\frac{\partial \psi_k}{\partial \mu}\right]\mathscr{D}^2\psi_{m-1-k} \\ &= (1-\mu^2)\sum_{i=0}^{k+1}\sum_{j=0}^{m-1-k} C_{k,i}(r)A_{m-1-k,j}(r)\mu^{i+j} \\ &= (1-\mu^2)\sum_{n=0}^{m}\mu^n\left(\sum_{i=\max\{0,n+k+1-m\}}^{\min\{k+1,n\}} C_{k,i}(r)A_{m-1-k,n-i}(r)\right). \end{aligned} \tag{A.17}$$

So, according to (A.9), (A.10), (A.11) and (A.12), we have for $0 \leqslant k \leqslant m-1$ that

$$\begin{aligned} &\frac{\partial \psi_k}{\partial r}\frac{\partial}{\partial \mu}(\mathscr{D}^2\psi_{m-1-k}) - \frac{\partial \psi_k}{\partial \mu}\frac{\partial}{\partial r}(\mathscr{D}^2\psi_{m-1-k}) \\ &= (1-\mu^2)\sum_{i=0}^{k}\sum_{j=0}^{m-k}[f'_{k,i}(r)T_{m-1-k,j}(r) - A'_{k,i}(r)S_{m-1-k,j}(r)]\mu^{i+j} \\ &= (1-\mu^2)\sum_{n=0}^{m}\mu^n\left(\sum_{i=\max\{0,n+k-m\}}^{\min\{k,n\}}[f'_{k,i}(r)T_{m-1-k,n-i}(r) - A'_{k,i}(r)S_{m-1-k,n-i}(r)]\right). \end{aligned} \tag{A.18}$$

By (A.17) and (A.18), it holds that

$$\sum_{k=0}^{m-1}\left[\frac{\partial\psi_k}{\partial r}\frac{\partial}{\partial\mu}-\frac{\partial\psi_k}{\partial\mu}\frac{\partial}{\partial r}+\frac{2\mu}{(1-\mu^2)}\frac{\partial\psi_k}{\partial r}+\frac{2}{r}\frac{\partial\psi_k}{\partial\mu}\right]\mathscr{D}^2\psi_{m-1-k}$$
$$=(1-\mu^2)\sum_{n=0}^{m}\mu^n\sum_{k=0}^{m-1}\left(\sum_{i=\max\{0,n+k+1-m\}}^{\min\{k+1,n\}}C_{k,i}(r)A_{m-1-k,n-i}(r)+\sum_{i=\max\{0,n+k-m\}}^{\min\{k,n\}}[f'_{k,i}(r)T_{m-1-k,n-i}(r)-A'_{k,i}(r)S_{m-1-k,n-i}(r)]\right). \quad (A.19)$$

Substituting (A.6), (A.19) into (2.22), we have by (2.25) and (2.29) that

$$G_m(r,\mu)=(1-\mu^2)\sum_{n=0}^{m}E_{m,n}(r)\mu^n, \quad (A.20)$$

where $E_{m,n}(r)$ $(0\leqslant n\leqslant m)$ is defined by

$$E_{m,n}(r)=(\hbar+\chi_m r^\sigma)\lambda_{m-1,n}B_{m-1,n}(r)-\frac{\hbar R_e}{r^2}\sum_{k=0}^{m-1}\left(\sum_{i=\max\{0,n+k+1-m\}}^{\min\{k+1,n\}}C_{k,i}(r)A_{m-1-k,n-i}(r)+\sum_{i=\max\{0,n+k-m\}}^{\min\{k,n\}}[f'_{k,i}(r)T_{m-1-k,n-i}(r)-A'_{k,i}(r)S_{m-1-k,n-i}(r)]\right). \quad (A.21)$$

By (2.25), (2.29), (A.6) and (A.20), Eq. (2.19) has the solution ψ_m, which can be expressed by the same mode expression as (A.1). Thus, (A.1) and therefore also (A.3) hold when $l=m$. Therefore, substituting (A.21) and (A.3) into (2.19), and then equating the term of power of μ, we have

$$f^{(4)}_{m,k}(r)-(k+1)(k+2)\left[\frac{2f''_{m,k}(r)}{r^2}-\frac{4f'_{m,k}(r)}{r^3}-(k-1)(k+4)\frac{f_{m,k}(r)}{r^4}\right]=\tilde{Q}_{m,k}(r) \quad (A.22)$$

with the boundary conditions

$$f_{m,k}(1)=f'_{m,k}(1)=0, \quad k=m,m-1,m-2,\ldots,1,0, \quad (A.23)$$

$$\lim_{r\to+\infty}r^{-2}f_{m,k}(r)=0, \quad k=m,m-1,m-2,\ldots,1,0, \quad (A.24)$$

where

$$\tilde{Q}_{m,k}(r)=\frac{E_{m,k}(r)}{r^\sigma}-2\lambda_{m,k+2}(k+1)(k+2)\left[\frac{f''_{m,k+2}(r)}{r^2}-2\frac{f'_{m,k+2}(r)}{r^3}\right]-\frac{(k+1)(k+2)(k+4)}{r^4}\times[(k+3)\lambda_{m,k+4}f_{m,k+4}(r)-2(k+1)\lambda_{m,k+2}f_{m,k+2}(r)]. \quad (A.25)$$

Multiplying (A.22) with r^4 gives

$$r^4f^{(4)}_{m,k}(r)-(k+1)(k+2)[2r^2f''_{m,k}(r)-4rf'_{m,k}(r)-(k-1)(k+4)f_{m,k}(r)]=Q_{m,k}(r), \quad r\geqslant 1, m\geqslant 1,\ 0\leqslant k\leqslant m, \quad (A.26)$$

where

$$Q_{m,k}(r)=r^{4-\sigma}E_{m,k}(r)-2\lambda_{m,k+2}(k+1)(k+2)\times[r^2f''_{m,k+2}(r)-2rf'_{m,k+2}(r)]-(k+1)(k+2)(k+4)\times[(k+3)\lambda_{m,k+4}f_{m,k+4}(r)-2(k+1)\lambda_{m,k+2}f_{m,k+2}(r)]. \quad (A.27)$$

They correspond to (2.31) and (2.34), respectively.

(III) Due to (I) and (II), mode expression (2.30) holds for every non-negative integer $m\geqslant 0$. This completes the proof.

Appendix B. Coefficients of drag formula (4.16) at the 10th-order of approximation

$\kappa_{10}^{1,2}=$
$+\,2.1027596574344023323615160349854\times 10^{-1}$,
$\kappa_{10}^{1,3}=$
$+\,1.6501530612244897959183673469387\times 10^{-1}$,

$$\kappa_{10}^{1,4} = + 8.2817528763399299113584827870542 1 \times 10^{-2},$$
$$\kappa_{10}^{1,5} = + 1.2754159580498866213151927437641 7 \times 10^{-2},$$
$$\kappa_{10}^{1,6} = - 1.6097864459674524609589544654479 7 \times 10^{-2},$$
$$\kappa_{10}^{1,7} = - 1.4540266834793736463495276111231 5 \times 10^{-2},$$
$$\kappa_{10}^{1,8} = - 5.9407905297991774015750039726063 7 \times 10^{-3},$$
$$\kappa_{10}^{1,9} = - 1.2897570146041540718292537901500 3 \times 10^{-3},$$
$$\kappa_{10}^{1,10} = - 1.2049347611230581201786467109379 4 \times 10^{-4},$$
$$\kappa_{10}^{2,4} = - 7.5755915832808721698669068925306 6 \times 10^{-3},$$
$$\kappa_{10}^{2,5} = - 4.6022866988634559728803199731574 6 \times 10^{-4},$$
$$\kappa_{10}^{2,6} = + 6.2364050312852575494332636979355 4 \times 10^{-4},$$
$$\kappa_{10}^{2,7} = + 2.6586401473252745712221785874668 8 \times 10^{-4},$$
$$\kappa_{10}^{2,8} = + 3.8118347263109652913064782536772 7 \times 10^{-5},$$
$$\kappa_{10}^{2,9} = - 1.9439178297932247367652333211831 5 \times 10^{-6},$$
$$\kappa_{10}^{2,10} = - 8.4548636370955687120285227573142 7 \times 10^{-7},$$
$$\kappa_{10}^{3,6} = + 7.2644851729309485849166142055411 0 \times 10^{-5},$$
$$\kappa_{10}^{3,7} = - 1.6036735236984585794413962706957 72 \times 10^{-5},$$
$$\kappa_{10}^{3,8} = - 4.5228948754071739642480230500236 55 \times 10^{-6},$$
$$\kappa_{10}^{3,9} = - 3.4721009330212440103424633495525 93 \times 10^{-7},$$
$$\kappa_{10}^{3,10} = + 3.5204473263645444185845428859181 61 \times 10^{-9},$$
$$\kappa_{10}^{4,8} = - 1.3061439805550873237485404802130 95 \times 10^{-7},$$
$$\kappa_{10}^{4,9} = + 3.6188982493712215937260532152992 52 \times 10^{-8},$$
$$\kappa_{10}^{4,10} = + 1.3573263795669288679431843303945 71 \times 10^{-9},$$
$$\kappa_{10}^{5,10} = + 1.2735228021789368770363990587013 15 \times 10^{-11}$$

References

[1] W. Chester, D.R. Breach, On the flow past a sphere at low Reynolds number, J. Fluid Mech. 37 (1969) 751–760.
[2] S. Goldstein, Concerning some solutions of the boundary layer equations in hydrodynamics, Proc. Cambridge Philos. Soc. 26 (1929).
[3] S.J. Liao, A kind of approximate solution technique which does not depend upon small parameters: an application in fluid mechanics, Int. J. Non-Linear Mech. 32 (1997) 815–822.
[4] S.J. Liao, A uniformly valid analytic solution of two dimensional viscous flow over a semi-infinite flat plate, J. Fluid Mech. 385 (1999) 101–128.
[5] S.J. Liao, An explicit, totally analytic approximate solution for Blasius' viscous flow problems, Int. J. Non-Linear Mech. 34 (1999) 759–778.
[6] S.J. Liao, A simple approach of enlarging convergence regions of perturbation approximations, Nonlinear Dynamics 19 (1999) 93–110.
[7] S.J. Liao, The general boundary element method and its further generalizations, Int. J. Numer. Methods Fluids 31 (1999) 627–655.
[8] T. Maxworthy, Accurate measurements of sphere drag at low Reynolds numbers, J. Fluid Mech. 23 (1965) 369–372.
[9] R. Ockendon, G.A. Evans, The drag on a sphere in low Reynolds number flow, J. Aerosol Sci. 3 (1972) 237–242.
[10] C.W. Oseen, Ueber die Stokessche Formel und die verwandte Aufgabe in der Hydrodynamik, Arkiv. Mat. Astron. Phsik. 6 (1910) 29.
[11] Proudman, J.R. Pearson, Expansion at small Reynolds number for the flow past a sphere and a circular cylinder, J. Fluid Mech. 2 (1957) 237–262.
[12] F.W. Roos, W.W. Willmarth, AIAA J. 9 (1971) 285–290.
[13] G.G. Stokes, Cambridge Philos. Trans. 9 (1851) 8.
[14] M. Van Dyke, J. Fluid Mech. 44 (1970) 365–372.
[15] M. Van Dyke, Turning a perturbation series upside down or inside out, in: T. Miloh (Ed.), Mathematical Approaches in Hydrodynamics, SIAM, Philadelphia, PA, 1991, pp. 473–477.
[16] F.M. White, Viscous Fluid Flow, McGraw-Hill, New York, 1991.
[17] N. Whitehead, Quart. J. Math. 23 (1889) 143.
[18] Wieselsberger, Phys. Z. 22 (1921) 321–328.
[19] Wieselsberger, Phys. Z. 23 (1921) 219–224.